Glycobiology, 2021, 1–11
doi: 10.1093/glycob/cwab014
Regular Manuscripts

Translational Glycobiology

NEU1 is more abundant in uveitic retina with concomitant desialylation of retinal cells

Lea Lorenz[2], Barbara Amann[2], Sieglinde Hirmer[2], Roxane L Degroote[2], Stefanie M Hauck[3] and Cornelia A Deeg[1,2]

[2]Chair of Physiology, Department of Veterinary Sciences, LMU Munich, Martinsried 82152, Germany, and [3]Research Unit Protein Science, Helmholtz Center Munich, German Research Center for Environmental Health (GmbH), Munich 80939, Germany

[1]To whom correspondence should be addressed: Tel: +49-89-2180-2552; Fax: +49-89-2180-2554; e-mail: Cornelia.Deeg@lmu.de

Received 7 August 2020; Revised 5 February 2021; Accepted 5 February 2021

Abstract

Desialylation of cell surface glycoproteins carried out by sialidases affects various immunological processes. However, the role of neuraminidase 1 (NEU1), one of the four mammalian sialidases, in inflammation and autoimmune disease is not completely unraveled to date. In this study, we analyzed the retinal expression of NEU1 in equine recurrent uveitis (ERU), a spontaneous animal model for autoimmune uveitis. Mass spectrometry revealed significantly higher abundance of NEU1 in retinal Müller glial cells (RMG) of ERU-diseased horses compared to healthy controls. Immunohistochemistry uncovered NEU1 expression along the whole Müller cell body in healthy and uveitic states and confirmed higher abundance in inflamed retina. Müller glial cells are the principal macroglial cells of the retina and play a crucial role in uveitis pathogenesis. To determine whether higher expression levels of NEU1 in uveitic RMG correlate with the desialylation of retinal cells, we performed lectin-binding assays with sialic acid-specific lectins. Through these experiments, we could demonstrate a profound loss of both α2-3- and α2-6-linked terminal sialic acids in uveitis. Hence, we hypothesize that the higher abundance of NEU1 in uveitic RMG plays an important role in the pathogenesis of uveitis by desialylation of retinal cells. As RMG become activated in the course of uveitis and actively promote inflammation, we propose that NEU1 might represent a novel activation marker for inflammatory RMG. Our data provide novel insights in the expression and implication of NEU1 in inflammation and autoimmune disease.

Key words: neuraminidase 1, retinal inflammation, retinal Müller glia, sialic acids, spontaneous autoimmune disease

Introduction

Modification of cell surface sialylation plays an important role in various immunological processes (Varki and Gagneux 2012; Läubli and Varki 2020). Desialylation of glycoproteins carried out by sialidases (also referred to as neuraminidases) impacts receptor activation, differentiation of immune cells and modulation of cell signaling and phagocytosis (Seyrantepe et al. 2010; Wang et al. 2016; Karmakar et al. 2019; Allendorf, Franssen, et al. 2020a; Allendorf, Puigdellívol, et al. 2020b).

Retinal Müller glial cells (RMG), the main macroglial cells of the retina, were described as cells actively participating in the inflammation by upregulating major histocompatibility complex II (MHC-II) molecules and secreting cytokines upon stimulation (Mano et al. 1991; Hauck et al. 2007; Bringmann et al. 2009; Rutar et al. 2015; Eastlake et al. 2016; Natoli et al. 2017; Capozzi et al. 2018). However, desialylation was not described in this context. RMG are considered accountable for maintaining the retinal ion-, water- and pH-homeostasis, providing neurons with nutrients and contributing

to the maintenance of the blood-retinal barrier (BRB) (Reichenbach and Bringmann 2020). Upon ocular inflammation, RMG transform into an activated gliotic state with upregulation of their intermediate filaments vimentin and glial fibrillary acidic protein (GFAP) and downregulation of cell-specific proteins like glutamine synthetase (GS), potassium channel Kir 4.1 and aquaporins 5 and 11 (Hauck et al. 2007; Bringmann et al. 2009; Eberhardt et al. 2011; Deeg et al. 2016).

As a severe intraocular inflammatory disease, uveitis is a major cause of visual impairment worldwide, eventually leading to blindness (Tsirouki et al. 2018). Equine recurrent uveitis (ERU) is the only spontaneous animal model for autoimmune uveitis (Wiedemann et al. 2020), and both diseases resemble each other in many aspects, such as clinical manifestations and immunopathology (Deeg et al. 2002). Besides, ERU has a high prevalence in the horse population (Malalana et al. 2015) and since affected retinas are readily available and can be collected and used immediately after enucleation, ERU represents an excellent animal model to study spontaneous disease pathogenesis (Deeg et al. 2008). Both in ERU and human autoimmune uveitis, autoreactive $CD4^+$ T-cells target retinal proteins, causing severe destruction of the retina (Caspi 2010; Wiedemann et al. 2020). In a previous study, primary RMG of ERU-diseased horses were shown to promote ocular inflammation by upregulating pro-inflammatory cytokine interferon γ (IFN)-γ (Hauck et al. 2007). Thus, RMG are supposed to play a decisive role in the pathogenesis of ocular inflammation, but the precise effects of RMG gliosis on uveitis pathogenesis remain to be elucidated. To gain further insight in the pathomechanisms underlying autoimmune uveitis and the role of RMG in the course of this sight-threatening disease, we analyzed primary RMG of healthy and ERU-diseased horses with differential proteome analysis and found a significant higher abundance of neuraminidase 1 (NEU1) in uveitic RMG.

NEU1 is an enzyme that cleaves terminal sialic acids from cell surface glycoproteins (Bonten et al. 1996). Thus, we were interested in how NEU1 impacts the sialylation state of retinal cells in this spontaneous model of autoimmune uveitis. It was shown that NEU1 is able to promote inflammation by desialylation of cell surface glycoproteins on immune cells such as macrophages and microglia (Amith et al. 2010; Karmakar et al. 2019; Allendorf, Franssen, et al. 2020a). Hence, the goal of this study was to corroborate the hypothesis that the higher abundance of NEU1 in uveitic RMG plays a significant role in the pathogenesis of uveitis by desialylation of retinal cells.

Results

Mass spectrometry reveals higher abundance of NEU1 and cathepsin A in an autoimmune disease

In a quantitative differential proteome analysis of RMG of healthy and ERU-diseased horses, we identified 172 proteins that were at least 1.8-fold more abundant in ERU and 345 proteins with a fold change of 0.6 or less in uveitic retina compared to healthy controls (Supplementary Table SI). Among the differentially abundant proteins was NEU1, which was 4-fold more abundant in RMG in uveitic state (Table I). Furthermore, cathepsin A (CTSA), a protease that associates with neuraminidase and is necessary for its stability and activity (van der Spoel et al. 1998; Bonten et al. 2014), was more abundant in uveitic RMG (Table I). We will refer to this protein in the following as protective protein cathepsin A (PPCA). Since the expression of NEU1 and PPCA in RMG was not described to date, we were interested to verify and further characterize their expression in RMG in general. Further, we wanted to investigate their implications in a spontaneous autoimmune disease model.

RMG express NEU1 and PPCA

NEU1 (Figure 1) and PPCA (Figure 2) expressions were first analyzed in the retinal tissue with immunohistochemistry of controls (Figures 1A and 2A, differential interference contrast image [DIC]) and ERU cases (Figures 1B and 2B). RMG marker vimentin indicated RMG localization and morphology, spanning the entire retina from the inner limiting membrane (ILM) to the outer limiting membrane (OLM) in both healthy (Figures 1C and 2C) and ERU-affected (Figures 1D and 2D) eyes. Expression pattern of vimentin in the control and uveitic sections resembled each other, indicating an early stage of disease and gliosis. Expression patterns of NEU1 displayed a RMG characteristic columnar shape in healthy (Figures 1E and 3A, left panel) and diseased (Figures 1F and 3A, right panel) retinas. However, in ERU, a stronger immunoreactivity for NEU1 became apparent (Figures 1F and 3A, right panel). Overlay images of vimentin and NEU1 confirmed respective Müller cell association of NEU1 (yellow) both in healthy (Figure 1G) and uveitic (Figure 1H) retinas (this figure is available in black and white in print and in color at *Glycobiology* online). PPCA expression could be detected in the different layers of the retina in healthy (Figures 2E and 3C, left panel) and uveitic (Figures 2F and 3C, right panel) states. Expression pattern of PPCA in the ILM and ganglion cell layer (GCL) revealed localization in RMG endfeet and trunks with their cell processes, but expression was also observed in a more punctate pattern in the INL and especially in the outer plexiform layer (OPL). Furthermore, the OLM stained heavily for PPCA. In the uveitic state (Figures 2F and 3C, right panel), a slight increase of immunoreactivity became apparent with the expression of PPCA also in the inner plexiform layer (IPL). Colocalization of vimentin and PPCA (yellow) was detected primarily in the RMG endfeet and trunks in the ILM and GCL both in healthy (Figure 2G) and uveitic retinas (Figure 2H) (this figure is available in black and white in print and in color at *Glycobiology* online).

NEU1 is significantly more abundant in RMG of uveitis cases

To verify the higher abundance of NEU1 in uveitis, NEU1 expression in RMG was quantified in healthy and diseased specimens (Figure 3). Quantification confirmed a significantly ($^{***}P \leq 0.001$) higher abundance of NEU1 (Figure 3B) in ERU cases (black column) compared to healthy controls (white column) (this figure is available in black and white in print and in color at *Glycobiology* online). By contrast, quantification of PPCA expression (Figure 3D) in the retina sections of healthy controls (white column) and uveitic cases with high expression levels of NEU1 (black column) revealed no significant difference ($P > 0.05$) (this figure is available in black and white in print and in color at *Glycobiology* online). As NEU1 efficiently cleaves sialic acid from glycoproteins (Bonten et al. 1996), we were next interested in whether the retinal cell surface sialylation was affected by the increased abundance of NEU1 in uveitic RMG.

Cell surface sialylation changes profoundly in uveitic retina

To substantiate changes in the cell surface sialylation in ERU, binding capacities of different lectins (Table II) in the retinal tissue of healthy (Figure 4A, DIC) and diseased (Figure 4B, DIC) horses were analyzed. DIC image revealed a slight thickening of the ILM concomitant with

Table I. Differential expression of NEU1 and CTSA in healthy and ERU affected RMG

Protein name	Gene name	Accession number	Unique peptides	Ratio ERU/healthy
Neuraminidase 1	NEU1	ENSECAP00000016932	2	4.0
Cathepsin A	CTSA	ENSECAP00000003740	7	1.9

Table II. Preferred binding substrates of used lectins

Acronym	Lectin name	Preferred binding substrates	References
WGA	Wheat germ agglutinin	GlcNAc(β1-4GlcNAc(β1-4GlcNAc)), Neu5Ac, GalNAc	(Nagata and Burger 1974)
MAL	*Maackia amurensis* leukoagglutinin	Siaα2-3Galβ1-4GlcNAc, SO4-3-Galβ1-4GlcNAc	(Geisler and Jarvis 2011)
MAH	*Maackia amurensis* hemagglutinin	Siaα2-3Galβ1-3(+/− Sia α2-6)GalNAc, SO4-3-Galβ1-3(+/− Sia α2-6)Gal(NAc)	(Geisler and Jarvis 2011)
SNA	*Sambucus nigra* lectin	Siaα2-6Gal(NAc)	(Shibuya et al. 1987)

a thinner photoreceptor outer segment (POS) in uveitis (Figure 4B). Wheat germ agglutinin (WGA, binding to *N*-acetylglucosamine [GlcNAc] and to a lesser extent to sialic acid *N*-acetyl-neuraminic acid [Neu5Ac]) was used as a negative control and was strongly positive in the ILM and OLM and in the plexiform layers in healthy retinas (Figures 4C and 5A, left panel). ERU cases (Figures 4D and 5A, right panel) revealed a similar expression pattern without obvious change in binding capacity. *Maackia amurensis* leukoagglutinin (MAL) binding was detected in the IPL and OPL and the OLM in the healthy state (Figures 4E and 5B, left panel), illustrating α2-3-linked sialic acids in *N*-linked glycans. By contrast, in autoimmune disease, a decrease in α2-3-linked sialic acids became apparent (Figures 4F and 5B, right panel) specifically in the IPL. *Maackia amurensis* hemagglutinin (MAH), specific for α2-3-linked sialic acids in *O*-linked glycans, was positive in the ILM and OLM, the GCL and the plexiform layers in healthy retina (Figures 4G and 5C, left panel). In the uveitic state, α2-3-linked sialic acids almost completely disappeared from the ILM, the GCL and the IPL (Figures 4H and 5C, right panel). *Sambucus nigra* lectin (SNA), binding specifically to α2-6-linked sialic acids, showed strong immunoreactivity along the ILM and in retinal ganglion cells as well as in the nuclear layers in healthy retinas (Figures 4I and 5D, left panel). In the diseased state, a strong decrease of α2-6-linked sialic acids became apparent especially in the ILM (Figures 4J and 5D, right panel).

Binding capacity of sialic acid-binding lectins significantly decreases in uveitis

While WGA binding (Figure 5A), which served as a negative control, revealed no significant difference between healthy retinas (white column) and ERU cases (black column) (this figure is available in black and white in print and in color at *Glycobiology* online), there was a clear difference in the sialic acid-binding lectins in the autoimmune disease. Binding capacities of specifically sialic acid-binding lectins MAL (Figure 5B), MAH (Figure 5C) and SNA (Figure 5D) were significantly ($^{**}P \leq 0.01$ for MAL and MAH and $^{*}P \leq 0.05$ for SNA) decreased in ERU (black column) compared to healthy controls (white column) (this figure is available in black and white in print and in color at *Glycobiology* online).

Discussion

In this study, we provide novel insights into the role of NEU1 in a spontaneous animal model for human autoimmune uveitis. We demonstrated that NEU1 is present in the equine retina in RMG (Table I, Figures 1 and 3) and also in retinal ganglion cells. Presence and activity of neuraminidase was reported in the chick retina (Dreyfus et al. 1976) and in bovine retinal rod outer segment membranes (Dreyfus et al. 1983). Here, we could show NEU1 expression in the equine retina throughout the whole Müller cell body from the ILM to the OLM (Figures 1E and F and 3A). Furthermore, mass spectrometry confirmed NEU1 expression in RMG (Table I) and in addition revealed the expression of PPCA (Table I), which is necessary for the stability and enzymatic activity of NEU1 (van der Spoel et al. 1998; Bonten et al. 2014).

Since the implications of NEU1 on autoimmune uveitis are unknown to date, we further analyzed NEU1 expression levels in uveitic retina. We detected a significantly higher abundance of NEU1 in uveitic RMG (Figure 3B), whereas PPCA abundance in RMG did not significantly increase in the course of disease (Figure 3D). Cathepsins are present in different localizations in the eye. Expression of PPCA was shown in mouse or rat cornea, pupil, lens, retinal pigment epithelium and in the optic nerve (Im and Kazlauskas 2007). While cathepsins seem to play a homeostatic role in the healthy eye, they were associated with the degradation of proteins and promotion of inflammation in pathological conditions (Im and Kazlauskas 2007). In this study, we report evidence for PPCA expression in the RMG of the equine retina by mass spectrometric analysis (Table I) and immunohistochemical assays (Figures 2E and F and 3C). However, in uveitis, higher expression levels of NEU1 were not accompanied by a higher abundance of PPCA (Figure 3D). Since we performed immunohistochemistry to analyze the overall PPCA protein abundance in equine retina, we cannot draw conclusions regarding potential differences in the activity of this enzyme between healthy and uveitic conditions with this method. To date, investigations on the interactions between PPCA and NEU1 had been performed in vitro with SV40-transformed simian cells (COS1 cells) (van der Spoel et al. 1998), insect cells (Bonten and d'Azzo 2000) and baculovirus-expressed wild-type and mutagenized recombinant enzymes and synthetic peptides (Bonten et al. 2009), but not in equine retinal cells. Therefore, this issue merits further investigation in the future.

As we previously demonstrated a pivotal role for RMG in uveitis pathogenesis (Hauck et al. 2007; Eberhardt et al. 2011; Deeg et al. 2016), we hypothesize that higher NEU1 abundance in RMG in this spontaneous autoimmune disease might play an important role in disease pathogenesis. In earlier studies, we showed that RMG actively contribute to inflammation, as they express IFN-γ in the uveitic

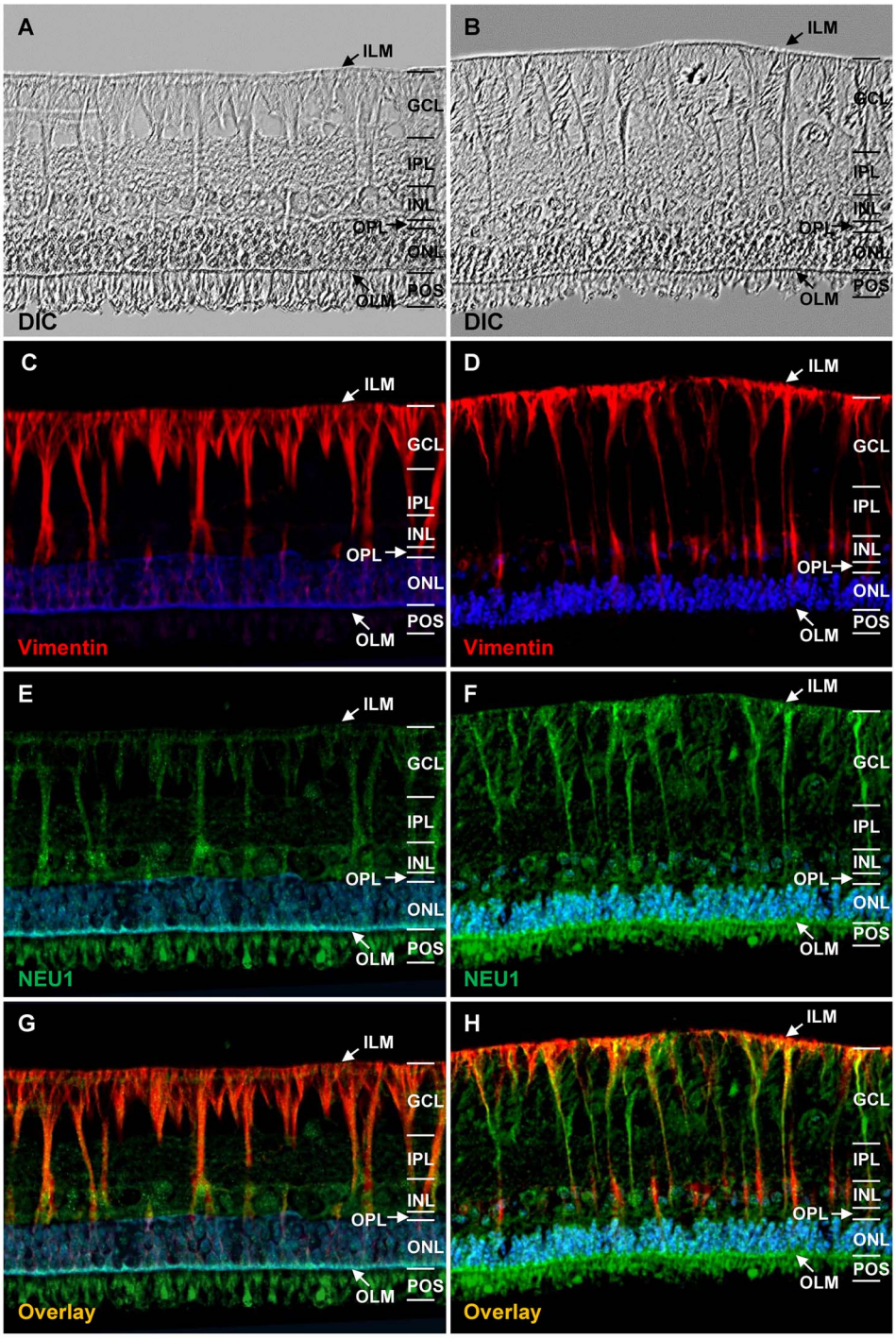

Fig. 1. RMG express NEU1 in healthy and uveitic state. DIC shows retinal structure in healthy (**A**) and uveitic (**B**) states. RMG marker vimentin (red) illustrated RMG localization and morphology within normal (**C**) and diseased (**D**) retinal tissue showing RMG characteristic columnar shape. Its expression pattern displayed only slight morphological changes of RMG in uveitic state (**D**), indicating the initial stage of gliosis. NEU1 expression pattern (green) revealed RMG morphology in both healthy (**E**) and diseased (**F**) state and higher abundance in uveitis (**F**). Double labeling (**G**, **H**) of vimentin (red) and NEU1 (green) confirmed NEU1 expression in RMG (colocalization yellow). ×400 magnification. Cell nuclei were counterstained with DAPI in blue.

state (Hauck et al. 2007). This is in line with the inflammatory potential of NEU1 that was demonstrated for different immune cells. In human T-lymphocytes, NEU1 expression and enzymatic activity increased upon the stimulation of the cells. Inhibition of this activity resulted in a significant reduction of IFN-γ production (Nan et al. 2007). We therefore speculate that a higher abundance of NEU1 in RMG is associated with the enhanced inflammation in uveitis. Also, in the human monocytic cell line THP-1, differentiation into macrophages was associated with increased NEU1 activity and concomitant loss of cell surface sialic acids (Wang et al. 2016). Thus,

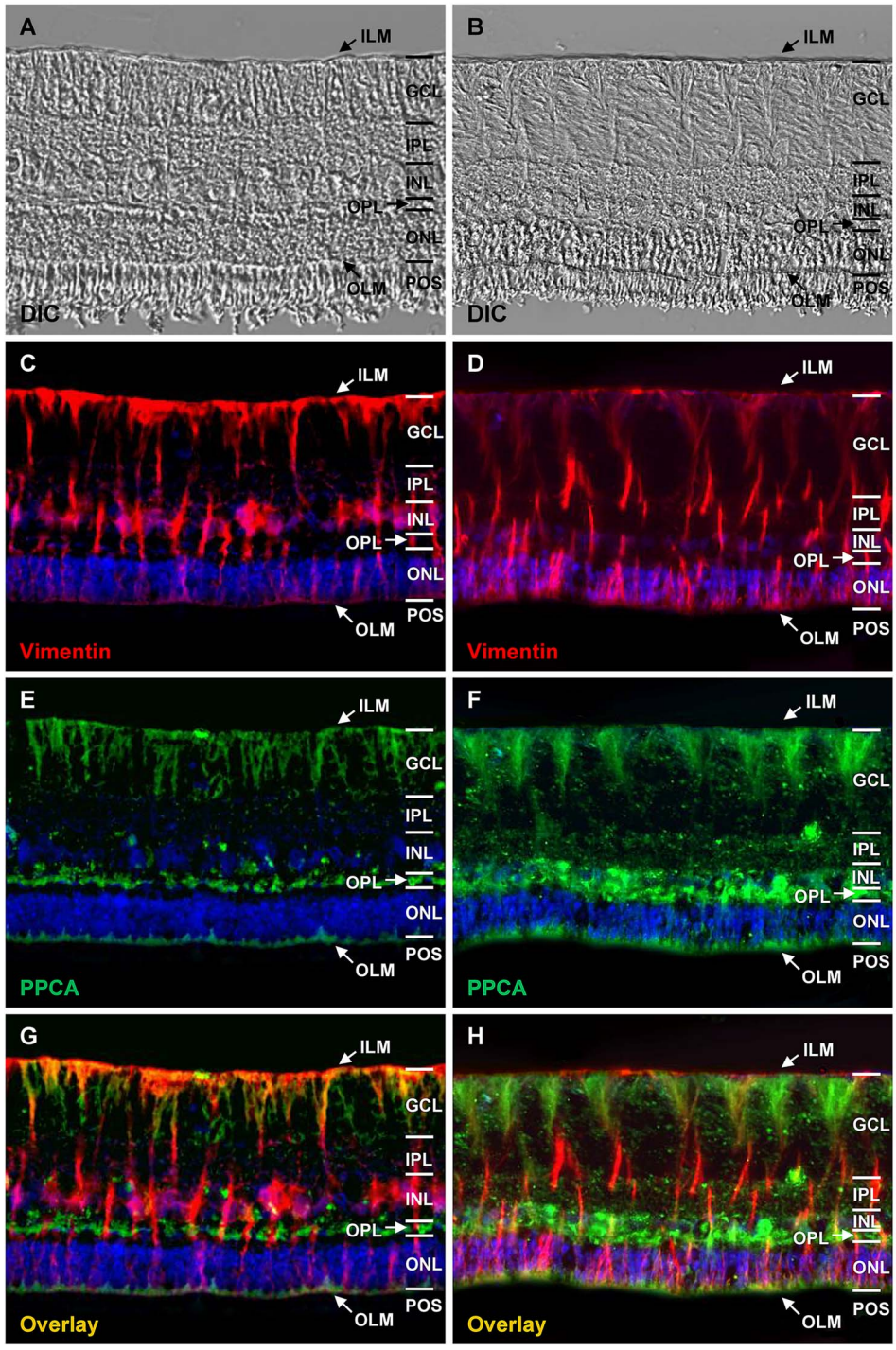

Fig. 2. PPCA is expressed in RMG in healthy and uveitic retina. DIC of representative healthy (**A**) and uveitic (**B**) retina sections reveals retinal architecture. Columnar expression pattern of intermediate filament vimentin (red) indicated RMG localization and morphology within healthy (**C**) and diseased (**D**) retinal tissue with signs of gliosis in uveitic state (**D**). PPCA expression (green) was detected especially in the GCL showing RMG characteristic shape and in the OPL and the OLM both in healthy (**E**) and diseased (**F**) retina. In uveitis (**F**), punctate expression increased especially in the IPL and INL. Overlay images of vimentin and PPCA demonstrate PPCA expression in RMG within healthy (**G**) and uveitic (**H**) retina (colocalization yellow). ×200 magnification. Cell nuclei were counterstained with DAPI in blue.

our data indicate that NEU1 might represent a new activation marker for inflammatory RMG.

NEU1 catalyzes the removal of α2-3- and α2-6-linked sialic acids from cell surface glycoproteins (Bonten et al. 1996). Hence, we were interested in the sialylation state of retinal tissue in healthy and uveitic eyes. We could demonstrate a significant loss of terminal α2-3- and α2-6-linked sialic acids in uveitis (Figures 4 and 5). Diminished α2-3-sialylation was particularly obvious in the

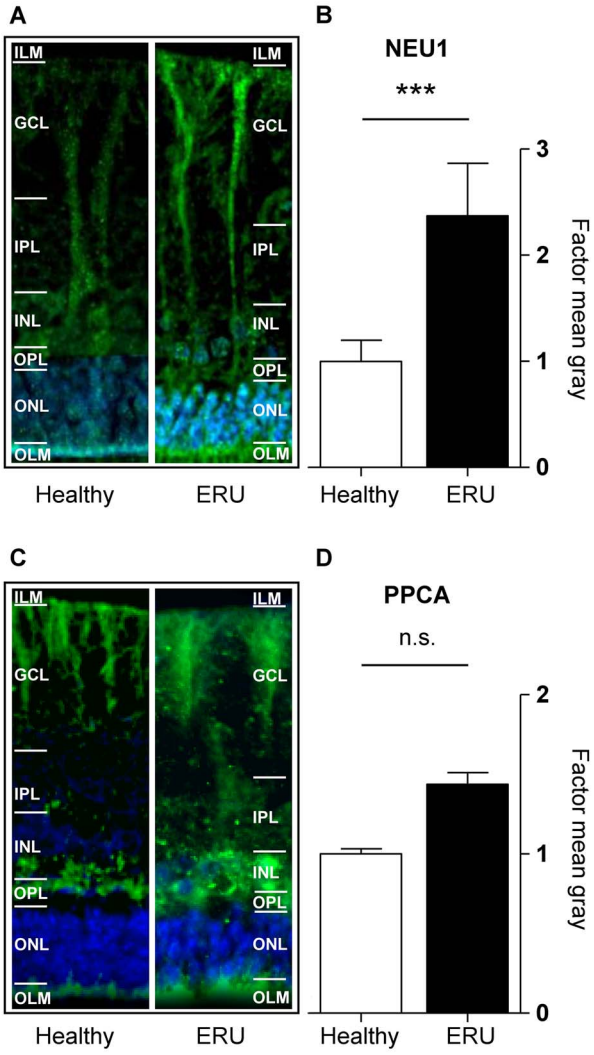

Fig. 3. NEU1 is more abundant in uveitic retina. Zoom-in images of Figure 1E and F show RMG (**A**) and illustrate increased expression of NEU1 throughout the cells in uveitis (right panel) compared to healthy controls (left panel). Quantification of fluorescence intensities of NEU1 (**B**) in immunohistochemical stainings of healthy (white column) and uveitic (black column) retinas revealed significantly higher expression levels of NEU1 in uveitic state compared to controls (***$P \leq 0.001$). Expression pattern of PPCA in RMG (**C**) is displayed in zoom-in images of Figure 2E and F for healthy (left panel) and uveitic (right panel) condition. Quantification of PPCA signal (**D**) did not yield a significant difference between healthy (white column) and diseased (black column) (n.s., $P > 0{,}05$).

IPL (Figures 4F and H and 5B and C). In the ILM, a loss of both α2-3- and α2-6-linked sialic acids became apparent in the uveitic state (Figures 4H and J and 5C and D). By contrast, binding of WGA, which served as a negative control since it binds primarily to GlcNAc and only to a small degree to the sialic acid Neu5Ac, was not significantly decreased (Figure 5A). These results indicate that the elevated expression of NEU1 in uveitis might result in decreased terminal sialylation of uveitic retinal cells. This is of major interest because the sialylation state of cells has an important impact on their functions (Varki and Gagneux 2012; Möckl 2020), and to our knowledge desialylation was not described in uveitis so far.

While interpreting our results, we have to keep in mind that there are other enzymes besides NEU1, regulating the sialylation state of cells. Sialidases NEU2, NEU3 and NEU4 also catalyze the cleavage of sialic acids, but they differ in substrate specificity, tissue expression and intracellular localization (Miyagi and Yamaguchi 2012). While glycoproteins are the main substrates of NEU1 (Bonten et al. 1996; Miyagi and Yamaguchi 2012), NEU3 preferentially cleaves sialic acids from gangliosides (Kopitz et al. 1996; Hasegawa et al. 2000). Since the organic solvents we used for the preparation of retina sections extract glycosphingolipids, such as gangliosides (Schwarz and Futerman 1997), we can conclude that in our experiments we demonstrated the cleavage of sialic acids from glycoproteins. However, we cannot exclude that gangliosides become desialylated as well in the course of ERU by NEU3. Since the retina exhibits a very diverse and unique ganglioside profile (Sibille et al. 2016) and the catabolization of gangliosides through NEU3 has important functions in the nervous system (Pan et al. 2017), these questions need to be addressed in future studies. Besides neuraminidases, sialyltransferases also play an essential role in regulating cell surface sialylation by catalyzing the transfer of sialic acid residues to the terminal position of glycoconjugates (Harduin-Lepers et al. 1995), thus having an opposite function to sialidases. This might explain, why in some parts of the retina, like the OLM, we observed a strong immunoreactivity for NEU1 in ERU (Figure 1F) without an apparent decrease of sialic acids (Figures 4 and 5). This phenomenon might be due to a higher expression or activity of sialyltransferases. However, our proteomic data revealed no higher abundance of sialyltransferases in RMG (Supplementary Table SI), but it cannot be excluded that other cell types of the retina contribute to the sialylation of cells by expressing sialyltransferases. While in the equine retina, NEU1 is primarily expressed in RMG (Figure 1), desialylation was not observed specifically in RMG, but throughout the retinal tissue (Figure 4). Since RMG span the entire thickness of the retina and are in close contact to the retinal neurons with their cell processes, it is reasonable to suggest that NEU1 on the cell surface of RMG could participate in the desialylation of the neighboring retinal cells. To date, this effect was not investigated in RMG and ocular diseases, but it was shown for other cells. Both in vivo and in vitro, NEU1 from activated polymorphonuclear leukocytes (PMNs) desialylated the surface of endothelial cells (ECs), resulting in the increased adhesion of PMN to the endothelium (Cross et al. 2003; Sakarya et al. 2004). Another explanation might be that retinal cells other than RMG express sialidases and thereby also contribute to the desialylation in uveitis. Which retinal cell types become desialylated in the course of uveitis and the direct substrate targets of NEU1 in the retina remain to be elucidated in future studies.

In uveitis, the consequences of retinal desialylation are unknown to date. It is conceivable that NEU1 could possibly mark an inflammatory phenotype of RMG, which leads to a pro-inflammatory microenvironment within the retina in ERU. Since immune cell activation and migration and destruction of the retinal tissue are the hallmarks of uveitis (Wiedemann et al. 2020), further attention should be paid to the potential role of desialylation in uveitis carried out by NEU1.

Furthermore, we hypothesize that the changes in retinal cell surface sialylation might impact the migration of immune cells. In uveitis, autoreactive T-cells migrate through the retina to the vitreous (Degroote et al. 2017). RMG abut to the ILM with their endfeet, thereby building the vitreo-retinal border that connects the retina and the vitreous body (Reichenbach and Bringmann 2020). Here, we have shown decreased α2-3- and α2-6-sialylation in uveitic

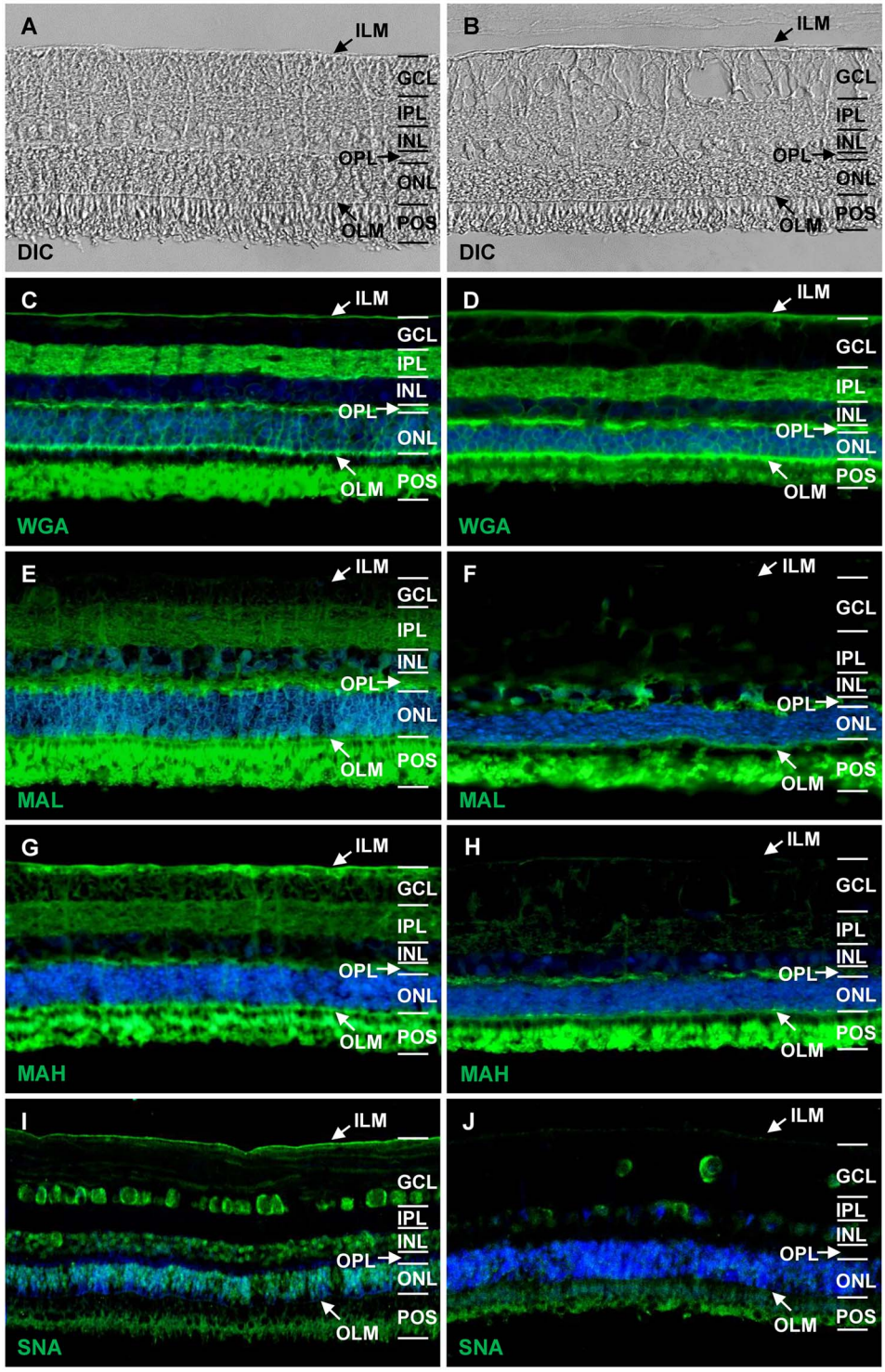

Fig. 4. Different binding patterns of lectins in healthy and uveitic retina indicate changes in surface sialylation. DIC of normal (**A**) and uveitic (**B**) retina with slightly damaged retinal structures in uveitic state (**B**). WGA (green), binding to GlcNAc and in a lesser extent to sialic acid, stained the limiting membranes and the plexiform layers (**C**, **D**) without apparent changes in uveitic retina (**D**). MAL (green) binds to α2-3-linked sialic acids in *N*-linked glycans and showed strong immunoreactivity in both plexiform layers and the OLM in healthy retina (**E**). In uveitis, α2-3-linked sialic acids were still detectable in the OPL and OLM, but almost completely disappeared in the IPL (**F**). MAH (green), binding to α2-3-linked sialic acids in *O*-linked glycans, revealed strong binding capacity in the ILM, GCL, IPL and OPL in healthy controls (**G**), whereas in diseased state, α2-3-linked sialic acids clearly decreased in the ILM, GCL and IPL (**H**). SNA (green), specific for α2-6-linked sialic acids, was strongly positive in the ILM and in retinal ganglion cells as well as in the nuclear layers in healthy state (**I**). By contrast, α2-6-linked sialic acids strongly decreased in uveitis, especially in the ILM (**J**). $\times$400 magnification. Cell nuclei were counterstained with DAPI in blue.

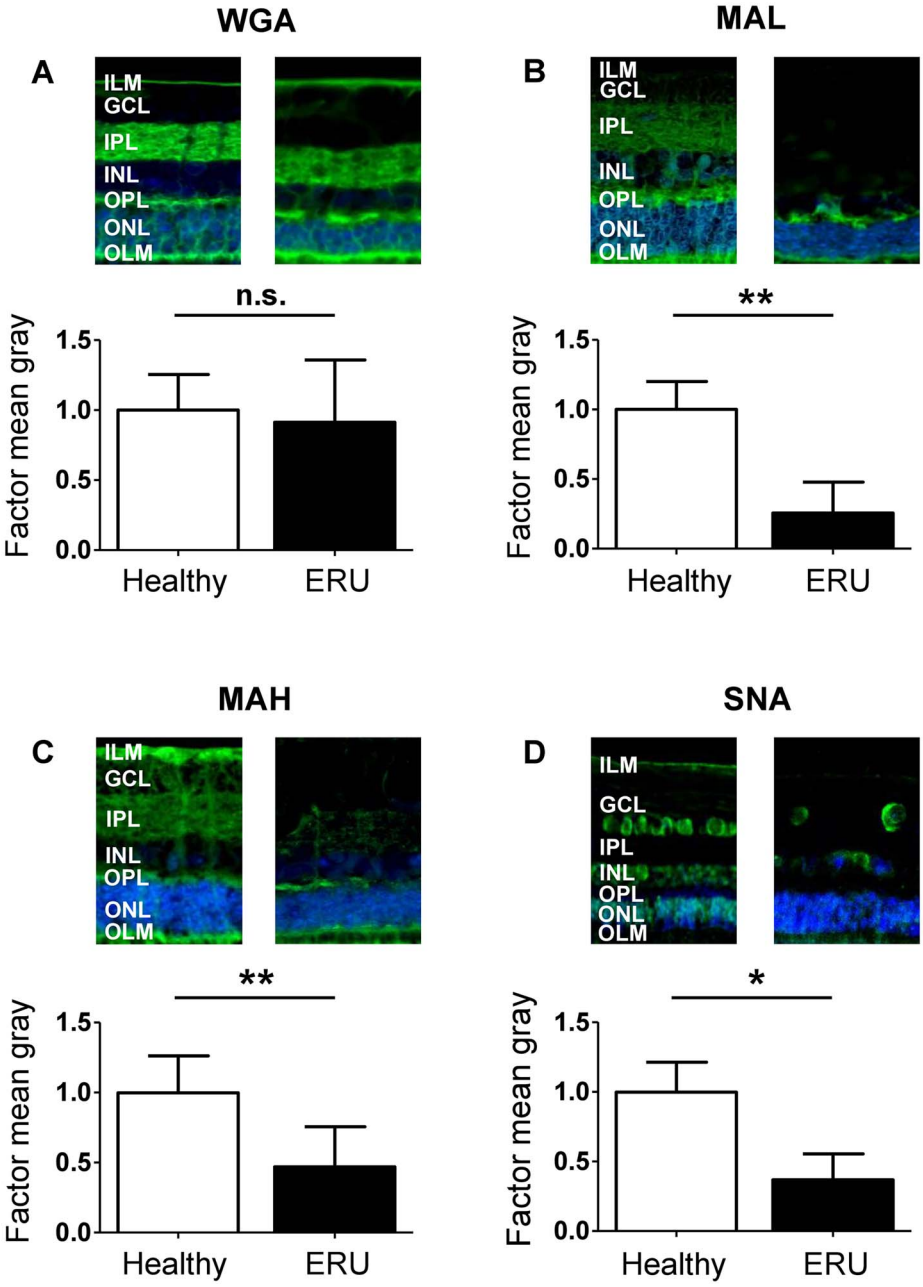

Fig. 5. Lectins MAL, MAH and SNA show significantly lower binding capacity in uveitis in contrast to WGA. Fluorescence intensity of WGA (**A**), which was used as a negative control, revealed no significant difference between healthy (white column) and uveitic (black column) retina (n.s., $P > 0.05$). By contrast, quantification of fluorescence intensities of sialic acid-binding lectins MAL (**B**), MAH (**C**) and SNA (**D**) confirmed a significant ($^{**}P \leq 0.01$ for MAL and MAH and $^{*}P \leq 0.05$ for SNA) decrease in uveitis (black columns) compared to healthy controls (white columns). Above the graphs, zoom-in images of respective lectin assays as shown in Figure 4 illustrate the decrease in binding capacity of sialic acid-binding lectins in uveitis (right panels) compared to healthy controls (left panels).

retina, especially at the ILM (Figures 4H and J and 5C and D). This could be in association with the transmigration of immune cells through the retinal tissue toward the vitreous. Loss of cell surface sialylation of retinal cells might attract immune cells and enhance their migratory capacity. In PMNs, enhanced migration is associated with endogenous sialidase activity that results in the desialylation of PMNs and ECs and therefore promotes the adhesion of PMNs to the endothelium (Feng et al. 2011). Thus, activated immune cells in uveitis might adhere more efficiently to desialylated retinal cells, resulting in an enhanced transmigration rate through retinal tissue.

Findings in this study came from the biological replicates from a spontaneous disease, therefore the samples display the heterogeneity of retinal inflammation. Our data are of special value, since we analyzed RMG in their natural retinal surrounding. Rather than western blot, we preferred immunohistochemistry of retina sections for the analysis and quantification of NEU1, PPCA and lectin binding. This is based on the fact that freshly isolated primary RMG from ERU

horses, which in this case are the sample of choice for quantification via western blot, are hard to obtain and scarcely available. The use of retinal whole cell lysates for western blot analysis is not adequate in this case as it does not allow to clearly distinguish the changes of protein abundance between RMG and other retinal cells. Using immunohistochemistry, we could differentiate between the changes that occur specifically in RMG from the changes that relate to other retinal cells. Thus, the significant differences in the NEU1 expression levels and α2-3- and α2-6-sialylation between healthy and uveitic retina suggest an essential role of these modifications in uveitis pathogenesis. In summary, our data point to a significant role of NEU1 expression changes in uveitic retina and concomitant desialylation of retinal cells.

Materials and methods

Retinal samples

For this study, a total of 15 control eyes and 12 ERU-diseased eyes were used. In detail, four control eyes and one ERU case were used for the separation of primary RMG and differential proteome analyses. Eleven control eyes and 12 ERU-diseased eyes from our tissue-biobank were used for immunohistochemistry (Deeg et al. 2016). Collection and use of equine eyes from the abattoir was approved for the purposes of scientific research by the appropriate board of the veterinary inspection office Munich, Germany (permit number: DE 09 162 0008-21). ERU specimens were derived from horses that were enucleated in the course of a therapeutical process in the equine hospital of LMU Munich or that had to be euthanized due to causes unrelated to this study. ERU was diagnosed based on the characteristic clinical signs of uveitis and a documented history of multiple recurrent episodes of ocular inflammation (Wollanke et al. 2001). All animals were treated according to the ethical principles and guidelines for scientific experiments on animals according to the ARVO statement for the use of animals in ophthalmic and vision research. No experimental animals were used in this study.

Sample preparation

Immediately after enucleation, eyecups were processed and the retina was dissected for the preparation of primary RMG as described previously (Eberhardt et al. 2012). Briefly, eyecups were cut open circumferentially and the anterior parts of the eye were removed. Retina was carefully detached from the vitreous residues and attached pigment epithelium. Mechanical disintegration of the retinal tissue was accomplished using micro-scissors, and the resulting fragments were enzymatically digested with papain (Carl Roth, Karlsruhe, Germany) for 30 min at 37°C. For enzyme activation, papain was incubated with 1.1 µM ethylenediaminetetraacetic acid (EDTA), 0.067 µM mercaptoethanol and 5.5 µM cysteine HCl prior to use. Enzymatical digestion was stopped by adding Dulbecco's modified Eagles Medium (DMEM, Pan Biotech, Aidenbach, Germany) with 10% of fetal bovine serum (FBS, Biochrom, part of Merck Millipore, Darmstadt, Germany). After the addition of desoxyribonuclease I (Sigma-Aldrich, Taufkirchen, Germany) and trituration, cells were collected by centrifugation. Subsequently, cells were resuspended and seeded into 25-cm^2 tissue flasks (Sarstedt, Nümbrecht, Germany) with DMEM containing 10% FBS and 1% penicillin/streptomycin (Pan Biotech). After allowing the cells to attach for 24 h, cells were purified through repeated washing and removal of the supernatant containing nonattached cells. Cells were cultured at 37°C and 5% CO_2.

For proteomic analysis, supernatant was completely removed and the attached cells were washed twice with phosphate buffered saline (PBS). Cells were lysed with lysis buffer containing 1% NP40, 10 mM NaCl and 10 mM tris-HCl (pH: 7.6) and were de-attached using a cell scraper. Lysed cells were stored at −20°C until further processing.

For immunohistochemical staining, posterior eyecups were sliced and were embedded in paraffin as described before (Ehrenhofer et al. 2002).

Mass-spectrometric analysis

Protein concentration was determined using Bradford protein assay (Bio-Rad AbD Serotec, Puchheim, Germany). From each sample, 10 µg of total protein was digested with LysC and trypsin by filter-aided sample preparation (FASP) as previously described (Grosche et al. 2016). Liquid chromatography coupled with tandem mass spectrometry (LC-MS/MS) analysis of digested samples was performed as previously described (Degroote et al. 2019). MS/MS spectra were subsequently searched against the Ensembl Horse protein database (release 89, Equ Cab 2, 24.849 sequences, http://www.ensembl.org) with Mascot (version 2.2, Matrix Science, http://www.matrixscience.com). Label-free quantification was performed with Progenesis software (version 2.5, Nonlinear Dynamics, Waters) as previously described (Hauck et al. 2017). Differential protein abundance was determined by the comparison of the mean normalized peptide abundance from the extracted ion chromatograms of ERU cases to controls.

Immunohistochemistry of retina sections

Paraffin-embedded tissues were sectioned (8 µm) and mounted on coated slides (Superfrost Plus, Thermo Fisher Scientific, Ulm, Germany). Heat antigen retrieval was performed at 99°C for 15 min in 0.1 M EDTA NaOH (pH 8.8) buffer. To prevent unspecific antibody binding, sections were blocked with TBS-T containing 1% bovine serum albumin (BSA) and 5% goat serum. Blocking serum was accordingly chosen to the species in which the secondary antibodies were produced. For candidate detection in tissue, we used monoclonal mouse antivimentin antibody (Sigma-Aldrich, 1:400), followed by secondary goat anti-mouse immunoglobulin G (IgG) H + L antibody coupled to Alexa Fluor 568 (Invitrogen, Karlsruhe, Germany, 1:500) and polyclonal rabbit antibody specific for human NEU1 (Thermo Fisher Scientific, 5 mg/mL, sequence homology of 93% for horse as given by the manufacturer) and human CTSA (Thermo Fisher Scientific, 1:100), respectively. High sequence homology for both antibodies was confirmed using BLASTP (https://blast.ncbi.nlm.nih.gov/Blast.cgi). In both cases, goat anti-mouse IgG H + L antibody coupled to Alexa Fluor 488 (Invitrogen, 1:500) was used as the secondary antibody. For staining with lectins, biotinylated MAL-I and MAL-II, here referred to as MAL and MAH, respectively (Geisler and Jarvis 2011), and fluorescein-labeled WGA and SNA (all Linaris, Dossenheim, Germany, 1 µg/mL) were used (Table II).

Target biotinylated lectins were visualized with fluorescein avidin D (Biozol, Eching, Germany, 10 µg/mL). Cell nuclei were counterstained with 4′,6-diamidino-2-phenylindole (DAPI, Invitrogen, 1:1000), and the sections were mounted with glass coverslips using fluorescent mounting medium (Serva, Heidelberg, Germany). Fluorescent images were recorded with the Leica DMi8 microscope and LASX software, version 3.4.2 (both Leica Microsystems, Wetzlar, Germany) was used for image processing.

Quantification of signal intensities

Fluorescence intensities of NEU1, PPCA and targets of lectins WGA, SNA, MAL and MAH in the immunohistochemical stainings of control samples and ERU cases were quantified using open source ImageJ 1.51 software (https://imagej.nih.gov/ij/). For quantification, factor mean gray was measured in representative areas, and the results were compared between healthy controls and ERU cases. Factor mean gray was used for statistical analysis of differences in staining intensity with Mann–Whitney *U* test (in case of no normal distribution) or Student's *t*-test (in case of normal distribution). Gaussian distribution was determined using the Kolmogorov–Smirnov test. Results were regarded as significant at $P \leq 0.05$. Significances were indicated by asterisks with $^{*}P \leq 0.05$, $^{**}P \leq 0.01$ and $^{***}P \leq 0.001$. Data were processed, analyzed and visualized using GraphPad Prism version 5.04 (GraphPad Software, San Diego, California) and OriginPro 2020 (Additive, Friedrichsdorf, Germany).

Supplementary data

Supplementary data for this article is available online at http://glycob.oxfordjournals.org/.

Acknowledgements

The authors would like to thank Nicole and Heinrich Veit for providing eye samples as well as Herbert Kaltner, Joachim Manning, Kristina Kleinwort and Claudia Barfüßer for critical discussions.

Funding

This work was supported by grants from the Deutsche Forschungsgemeinschaft in the SPP 2127, projects DFG DE 719/7-1 to C.D., HA 6014/5-1 to S.M.H.

Conflict of interest statement

The authors declare no conflict of interest.

Abbreviations

BRB, blood-retinal barrier; BSA, bovine serum albumin; DAPI, 4′,6-diamidino-2-phenylindole; DIC, differential interference contrast image; EC, endothelial cell; EDTA, ethylenediaminetetraacetic acid; ERU, equine recurrent uveitis; FASP, filter-aided sample preparation; GCL, ganglion cell layer; GFAP, glial fibrillary acidic protein; GlcNAc, *N*-acetylglucosamine; GS, glutamine synthetase; IFN-γ, interferon γ; IgG, immunoglobulin G; ILM, inner limiting membrane; INL, inner nuclear layer; IPL, inner plexiform layer; LC-MS/MS, liquid chromatography coupled with tandem mass spectrometry; MHC-II, major histocompatibility complex II; NEU1, neuraminidase 1; Neu5Ac, *N*-acetyl-neuraminic acid; OLM, outer limiting membrane; ONL, outer nuclear layer; OPL, outer plexiform layer; PBS, phosphate buffered saline; PMN, polymorphonuclear leukocytes; POS, photoreceptor outer segment; PPCA, protective protein cathepsin A; RMG, retinal Müller glial cells; SF, synovial fibroblast.

References

Allendorf DH, Franssen EH, Brown GC. 2020a. Lipopolysaccharide activates microglia via neuraminidase 1 desialylation of Toll-like Receptor 4. *J Neurochem*155:403-416.

Allendorf DH, Puigdellívol M, Brown GC. 2020b. Activated microglia desialylate their surface, stimulating complement receptor 3-mediated phagocytosis of neurons. *Glia*. 68:989–998.

Amith SR, Jayanth P, Franchuk S, Finlay T, Seyrantepe V, Beyaert R, Pshezhetsky AV, Szewczuk MR. 2010. Neu 1 desialylation of sialyl α-2, 3-linked β-galactosyl residues of TOLL-like receptor 4 is essential for receptor activation and cellular signaling. *Cell Signal*. 22:314–324.

Bonten E, van der Spoel A, Fornerod M, Grosveld G, d'Azzo A. 1996. Characterization of human lysosomal neuraminidase defines the molecular basis of the metabolic storage disorder sialidosis. *Genes Dev*. 10:3156–3169.

Bonten EJ, d'Azzo A. 2000. Lysosomal neuraminidase. Catalytic activation in insect cells is controlled by the protective protein/cathepsin A. *J Biol Chem*. 275:37657–37663.

Bonten EJ, Annunziata I, d'Azzo A. 2014. Lysosomal multienzyme complex: Pros and cons of working together. *Cell Mol Life Sci*. 71:2017–2032.

Bonten EJ, Campos Y, Zaitsev V, Nourse A, Waddell B, Lewis W, Taylor G, d'Azzo A. 2009. Heterodimerization of the sialidase NEU1 with the chaperone protective protein/cathepsin A prevents its premature oligomerization. *J Biol Chem*. 284:28430–28441.

Bringmann A, Iandiev I, Pannicke T, Wurm A, Hollborn M, Wiedemann P, Osborne NN, Reichenbach A. 2009. Cellular signaling and factors involved in Müller cell gliosis: Neuroprotective and detrimental effects. *Prog Retin Eye Res*. 28:423–451.

Capozzi ME, Giblin MJ, Penn JS. 2018. Palmitic acid induces Müller cell inflammation that is potentiated by co-treatment with glucose. *Sci Rep*. 8:5459.

Caspi RR. 2010. A look at autoimmunity and inflammation in the eye. *J Clin Invest*. 120:3073–3083.

Cross AS, Sakarya S, Rifat S, Held TK, Drysdale BE, Grange PA, Cassels FJ, Wang LX, Stamatos N, Farese A *et al*. 2003. Recruitment of murine neutrophils in vivo through endogenous sialidase activity. *J Biol Chem*. 278:4112–4120.

Deeg CA, Ehrenhofer M, Thurau SR, Reese S, Wildner G, Kaspers B. 2002. Immunopathology of recurrent uveitis in spontaneously diseased horses. *Exp Eye Res*. 75:127–133.

Deeg CA, Amann B, Lutz K, Hirmer S, Lutterberg K, Kremmer E, Hauck SM. 2016. Aquaporin 11, a regulator of water efflux at retinal Muller glial cell surface decreases concomitant with immune-mediated gliosis. *J Neuroinflammation*. 13:89.

Deeg CA, Hauck SM, Amann B, Pompetzki D, Altmann F, Raith A, Schmalzl T, Stangassinger M, Ueffing M. 2008. Equine recurrent uveitis—A spontaneous horse model of uveitis. *Ophthalmic Res*. 40:151–153.

Degroote RL, Weigand M, Hauck SM, Deeg CA. 2019. IL8 and PMA trigger the regulation of different biological processes in granulocyte activation. *Front Immunol*. 10:3064.

Degroote RL, Uhl PB, Amann B, Krackhardt AM, Ueffing M, Hauck SM, Deeg CA. 2017. Formin like 1 expression is increased on CD4+ T lymphocytes in spontaneous autoimmune uveitis. *J Proteomics*. 154:102–108.

Dreyfus H, Preti A, Harth S, Pellicone C, Virmaux N. 1983. Neuraminidase in calf retinal outer segment membranes. *J Neurochem*. 40: 184–188.

Dreyfus H, Harth S, Urban PF, Mandel P, Preti A, Lombardo A. 1976. On the presence of a "particle-bound" neuraminidase in retina. A developmental study. *Life Sci*. 18:1057–1063.

Eastlake K, Banerjee PJ, Angbohang A, Charteris DG, Khaw PT, Limb GA. 2016. Müller glia as an important source of cytokines and inflammatory factors present in the gliotic retina during proliferative vitreoretinopathy. *Glia*. 64:495–506.

Eberhardt C, Amann B, Feuchtinger A, Hauck SM, Deeg CA. 2011. Differential expression of inwardly rectifying K+ channels and aquaporins 4 and 5 in autoimmune uveitis indicates misbalance in Müller glial cell-dependent ion and water homeostasis. *Glia*. 59:697–707.

Eberhardt C, Amann B, Stangassinger M, Hauck SM, Deeg CA. 2012. Isolation, characterization and establishment of an equine retinal glial cell line: A prerequisite to investigate the physiological function of Muller cells in the retina. *J Anim Physiol Anim Nutr*. 96:260–269.

Ehrenhofer MCA, Deeg CA, Reese S, Liebich H-G, Stangassinger M, Kaspers B. 2002. Normal structure and age-related changes of the equine retina. *Vet Ophthalmol*. 5:39–47.

Feng C, Zhang L, Almulki L, Faez S, Whitford M, Hafezi-Moghadam A, Cross AS. 2011. Endogenous PMN sialidase activity exposes activation epitope on CD11b/CD18 which enhances its binding interaction with ICAM-1. *J Leukoc Biol*. 90:313–321.

Geisler C, Jarvis DL. 2011. Letter to the glyco-forum: Effective glycoanalysis with *Maackia amurensis* lectins requires a clear understanding of their binding specificities. *Glycobiology*. 21:988–993.

Grosche A, Hauser A, Lepper MF, Mayo R, von Toerne C, Merl-Pham J, Hauck SM. 2016. The proteome of native adult Müller glial cells from murine retina. *Mol Cell Proteomics*. 15:462–480.

Harduin-Lepers A, Recchi MA, Delannoy P. 1995. 1994, the year of sialyltransferases. *Glycobiology*. 5:741–758.

Hasegawa T, Yamaguchi K, Wada T, Takeda A, Itoyama Y, Miyagi T. 2000. Molecular cloning of mouse ganglioside sialidase and its increased expression in Neuro2a cell differentiation. *J Biol Chem*. 275:8007–8015.

Hauck SM, Lepper MF, Hertl M, Sekundo W, Deeg CA. 2017. Proteome dynamics in biobanked horse peripheral blood derived lymphocytes (PBL) with induced autoimmune uveitis. *Proteomics*. 17:1-5.

Hauck SM, Schoeffmann S, Amann B, Stangassinger M, Gerhards H, Ueffing M, Deeg CA. 2007. Retinal Mueller glial cells trigger the hallmark inflammatory process in autoimmune uveitis. *J Proteome Res*. 6:2121–2131.

Im E, Kazlauskas A. 2007. The role of cathepsins in ocular physiology and pathology. *Exp Eye Res*. 84:383–388.

Karmakar J, Roy S, Mandal C. 2019. Modulation of TLR4 sialylation mediated by a sialidase Neu1 and impairment of its signaling in *Leishmania donovani* infected macrophages. *Front Immunol*. 10:1-19.

Kopitz J, von Reitzenstein C, Sinz K, Cantz M. 1996. Selective ganglioside desialylation in the plasma membrane of human neuroblastoma cells. *Glycobiology*. 6:367–376.

Läubli H, Varki A. 2020. Sialic acid-binding immunoglobulin-like lectins (Siglecs) detect self-associated molecular patterns to regulate immune responses. *Cell Mol Life Sci*. 77:593–605.

Malalana F, Stylianides A, McGowan C. 2015. Equine recurrent uveitis: Human and equine perspectives. *Vet J*. 206:22–29.

Mano T, Tokuda N, Puro DG. 1991. Interferon-gamma induces the expression of major histocompatibility antigens by human retinal glial cells. *Exp Eye Res*. 53:603–607.

Miyagi T, Yamaguchi K. 2012. Mammalian sialidases: Physiological and pathological roles in cellular functions. *Glycobiology*. 22:880–896.

Möckl L. 2020. The emerging role of the mammalian glycocalyx in functional membrane organization and immune system regulation. *Front Cell Dev Biol*. 8:1-14.

Nagata Y, Burger MM. 1974. Wheat germ agglutinin. Molecular characteristics and specificity for sugar binding. *J Biol Chem*. 249: 3116–3122.

Nan X, Carubelli I, Stamatos NM. 2007. Sialidase expression in activated human T lymphocytes influences production of IFN-γ. *J Leukoc Biol*. 81:284–296.

Natoli R, Fernando N, Madigan M, Chu-Tan JA, Valter K, Provis J, Rutar M. 2017. Microglia-derived IL-1β promotes chemokine expression by Müller cells and RPE in focal retinal degeneration. *Mol Neurodegener*. 12:31.

Pan X, de Britto Pará de Aragão C, Velasco-Martin JP, Priestman DA, Wu HY, Takahashi K, Yamaguchi K, Sturiale L, Garozzo D, Platt FM *et al*. 2017. Neuraminidases 3 and 4 regulate neuronal function by catabolizing brain gangliosides. *FASEB J*. 31:3467–3483.

Reichenbach A, Bringmann A. 2020. Glia of the human retina. *Glia*. 68:768–796.

Rutar M, Natoli R, Chia RX, Valter K, Provis JM. 2015. Chemokine-mediated inflammation in the degenerating retina is coordinated by Müller cells, activated microglia, and retinal pigment epithelium. *J Neuroinflammation*. 12:8.

Sakarya S, Rifat S, Zhou J, Bannerman DD, Stamatos NM, Cross AS, Goldblum SE. 2004. Mobilization of neutrophil sialidase activity desialylates the pulmonary vascular endothelial surface and increases resting neutrophil adhesion to and migration across the endothelium. *Glycobiology*. 14:481–494.

Schwarz A, Futerman AH. 1997. Determination of the localization of gangliosides using anti-ganglioside antibodies: Comparison of fixation methods. *J Histochem Cytochem*. 45:611–618.

Seyrantepe V, Iannello A, Liang F, Kanshin E, Jayanth P, Samarani S, Szewczuk MR, Ahmad A, Pshezhetsky AV. 2010. Regulation of phagocytosis in macrophages by neuraminidase 1. *J Biol Chem*. 285: 206–215.

Shibuya N, Goldstein IJ, Broekaert WF, Nsimba-Lubaki M, Peeters B, Peumans WJ. 1987. The elderberry (*Sambucus nigra* L.) bark lectin recognizes the Neu5Ac(alpha 2-6) Gal/GalNAc sequence. *J Biol Chem*. 262: 1596–1601.

Sibille E, Berdeaux O, Martine L, Bron AM, Creuzot-Garcher CP, He Z, Thuret G, Bretillon L, Masson EA. 2016. Ganglioside profiling of the human retina: Comparison with other ocular structures, brain and plasma reveals tissue specificities. *PLoS One*. 11: 1-22.

Tsirouki T, Dastiridou A, Symeonidis C, Tounakaki O, Brazitikou I, Kalogeropoulos C, Androudi S. 2018. A focus on the epidemiology of uveitis. *Ocul Immunol Inflamm*. 26:2–16.

van der Spoel A, Bonten E, d'Azzo A. 1998. Transport of human lysosomal neuraminidase to mature lysosomes requires protective protein/cathepsin A. *EMBO J*. 17:1588–1597.

Varki A, Gagneux P. 2012. Multifarious roles of sialic acids in immunity. *Ann N Y Acad Sci*. 1253:16–36.

Wang D, Ozhegov E, Wang L, Zhou A, Nie H, Li Y, Sun X-L. 2016. Sialylation and desialylation dynamics of monocytes upon differentiation and polarization to macrophages. *Glycoconj J*. 33:725–733.

Wiedemann C, Amann B, Degroote RL, Witte T, Deeg CA. 2020. Aberrant migratory behavior of immune cells in recurrent autoimmune uveitis in horses. *Front Cell Dev Biol*. 8:101.

Wollanke B, Rohrbach BW, Gerhards H. 2001. Serum and vitreous humor antibody titers in and isolation of *Leptospira interrogans* from horses with recurrent uveitis. *J Am Vet Med Assoc*. 219:795–800.